ACS OMEGA

http://pubs.acs.org/journal/acsodf

Article

Novel Core/Shell Nylon 6,6/La-TMA MOF Electrospun Nanocomposite Membrane and CO_2 Capture Assessments of the Membrane and Pure La-TMA MOF

Zohreh Fateminia,* Hossein Chiniforoshan, and Vahid Ghafarinia

Cite This: *ACS Omega* 2023, 8, 22742−22751

Read Online

ACCESS | Metrics & More | Article Recommendations | Supporting Information

ABSTRACT: Membrane technology plays a vital, applicable, and essential role in human life and industry. The high adsorption capacity of membranes can be employed for capturing air pollutants and greenhouse gases. In this work, we tried to develop a shaped industrial form of a metal−organic framework as an adsorbent material with the ability to capture CO_2 in the laboratory phase. To do so, a core/shell Nylon 6,6/La-TMA MOF nanofiber composite membrane was synthesized. This organic/inorganic nanomembrane is a kind of nonwoven electrospun fiber that was prepared using the coaxial electrospinning approach. FE-SEM, surface area calculations, nitrogen adsorption/desorption, XRD grazing incidence on thin films, and histogram diagrams were applied to assess the quality of the membrane. This composite membrane as well as pure La-TMA MOF were assessed as CO_2 adsorbent materials. The CO_2 adsorption abilities of the core/shell Nylon 6,6/La-TMA MOF membrane and pure La-TMA MOF were as high as 0.219 and 0.277 mmol/g, respectively. As a result of preparing the nanocomposite membrane from microtubes of La-TMA MOF, the %A of the micro La-TMA MOF (% 43.060) increased to % 48.524 for Nylon 6,6/La-TMA MOF.

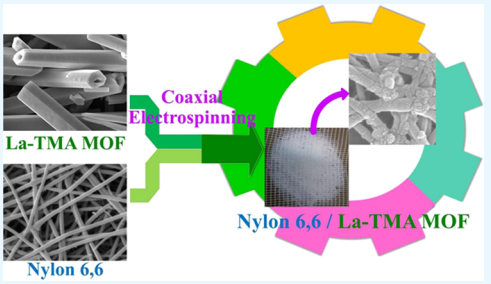

1. INTRODUCTION

Metal−organic frameworks (MOFs) constitute one of the most notable materials in chemistry and some other scientific areas. Their excellent structures, great architecture, and long-coordination modes bestow them with very unique features. Therefore, they constitute one of the most engaging branches of materials science and chemistry.

CO_2 is a crucial greenhouse gas that retains the warmth of the earth's surface. Without CO_2, this temperature would have been −18 °C, but with CO_2, it increased to about 15 °C. The basic problem correlated to greenhouse gases, especially CO_2, is their excessive amount in the air, mainly because of industrial activity and the combustion of fossil fuels. Before the industrial revolution, the CO_2 concentration was below 280 ppm, while in 2019, it became about 410 ppm.[1]

At present, in industry and laboratories, carbon oxide is adsorbed through special solvents, solid adsorbents, membranes, ionic liquids, MOFs, polymeric membranes comprising composite electrospun nanofiber membranes, etc.[2]

Research and publication on CO_2 capture started about half a century ago, in 1975.[3] For the first time, MOFs were applied for CO_2 adsorption by Yaghi's group in 1998.[4]

Regeneration, conversion, and capture of CO_2 have high importance not only because of its greenhouse effects but also due to the overabundance of C1 as a building block in organic transformation reactions as well as its free availability, renewability, and nontoxic properties.[5,6]

Generally, there are three main methods to reduce CO_2 in the industry: oxyfuel combustion, post-combustion, and pre-combustion. In the post-combustion approach, CO_2 is captured after the combustion of fossil fuels or other fuels that produce CO_2. In some cases, the existence of impurities, for example in natural gas, causes an unclean flue gas stream, and subsequently, additional clean-up and CO_2 capture are needed. However, CO_2 capture is currently carried out through chemical adsorption in aqueous organic-based solutions, such as mono- or diethanol amines.[7]

CO_2 adsorption technology is mostly based on solvents and liquid phases in comparison with highly porous metal−organic frameworks in the solid phase.[8]

Polymeric membranes are extensively applied in the industry and in daily life because of their solution processability and flexibility. Polymeric membranes can purify special types of pollutant gases through selectivity or permeability mechanisms.[9]

The first industrial application of a membrane to separate components from a mixture of gases was achieved in about 1980 to collect hydrogen gas.[10]

Received: March 9, 2023
Accepted: May 30, 2023
Published: June 13, 2023

In the last few years, several composites comprising various polymers as well as inorganic materials have been introduced as mixed matrix membranes (MMMs) to separate/adsorb several-component mixtures; these membranes are composed of a homogeneous combination of inorganic particles in a polymeric matrix, which forms the base of the mixed matrix membrane.[7] MMMs have noticeable properties such as the ability to separate a mixture of different components in the liquid or gaseous phase; furthermore, flexibility is another vital property of these membranes.[11] Zeolites, activated carbon, carbon nanotubes, silica gel, mesoporous silica, nonporous materials, and especially metal−organic frameworks constitute inorganic fillers applied for preparing MMMs. However, metal−organic frameworks are the latest class in this group.[7,12]

In recent decades, membrane technology has attracted great attention, especially in fuel cells, industrial energy-efficient separation, drug delivery, dialysis devices, and so on, because of their role as selective barriers. At present, membrane processes play vital roles in some industrial areas such as CO_2 capture from flue gas or CO_2 elimination from natural gas. Membranes are composed of organic/polymeric compounds and inorganic materials, which are designed for specific purposes, depending on the cost of the precursors, processability, thermal/chemical stability, and other desirable properties.

An increase in the permeability of a membrane leads to a decrease in selectivity; however, inorganic membranes have high permeability and selectivity because of their porous nature. Because of the complex processability and price of pure inorganic membranes, inorganic materials composed of silica, zeolites, metals, metal oxides, activated carbon, carbon molecular sieves, and especially advanced porous materials including metal−organic frameworks (MOFs), covalent organic frameworks (COFs), porous organic cages (POCs), together with organic polymers, are expected to have synergistic effects. In order to separate different components of an aqueous/gaseous mixture, microporous materials (with pore diameters <2 nm) are more suitable due to the similarity in pore diameters and kinetic diameters of the gas/liquid, which leads to an increase in the probability of size-selective separation.[13]

Some examples of separating/purifying mixtures of components through metal−organic frameworks or their mixed membranes are given here. The CO_2 adsorption of an MOF-based suspension of ZIF-8 in an ionic liquid was measured by Liu et al. The CO_2 capture of this suspension was about 2.5 mg/g (0.0568 mmol/g) at 298 K.[8] In order to control the release of picaridin, a composite of Nylon 6,6 and this insect repellent was used and studied by Ryan and co-workers.[14] Nylon 6,6/graphene oxide and Nylon 6/UiO-66-NH_2 nanofiber composites were used to remove toxic Cr (VI) with suitable capacities.[15,16] Nylon 6/chitosan core/shell nanofibers, as the antibacterial product, were synthesized, applied, and assessed to inhibit infections of surgical trauma by Keirouz et al.[17]

In Table 1, decomposition temperatures of some common organic polymers in the form of pellets/powder and fibers are compared.[18]

In the CO_2 capture process, four strategies are pursued: (a) post-combustion capture, (b) pre-combustion capture, (c) direct air capture, and (d) oxyfuel combustion. CO_2 removal from flue gas, after combustion of natural gas, represents the "post-combustion CO_2 capture" process.[19]

Table 1. Onset Decomposition Temperatures of PMMA, PVC, Nylon 6, and Nylon 6,6[18]

polymer	onset decomposition temperature (°C)
PMMA electrospun	306
PMMA powder	266
PVC electrospun	276
PVC powder	282
Nylon 6 electrospun	424
Nylon 6 pellets	408
Nylon 6,6 electrospun	424
Nylon 6,6 pellets	434

Zeolites (porous aluminosilicate materials with a solid phase) in comparison with alkanolamine solutions exhibit faster CO_2 capture and less energy dissipation in degassing procedures, whereas their usage is limited by a low adsorption capacity and instability in the presence of water. Moreover, activated carbon with a high CO_2 adsorption capacity, especially under high pressure, has low CO_2/N_2 selectivity.[19]

In Table 2, some cases of metal−organic frameworks or their mixed membranes and their CO_2 adsorption ability under various conditions are given. Introducing metal−organic frameworks with an extensive diversity of pores and a high surface area opens a new window in several scientific branches to scientists.[19] The CO_2 capture capacity of MOFs in bulk is not necessarily more than that of MOFs incorporated into membranes.[20]

Table 2. Some Metal−Organic Frameworks or their Mixed Membranes and their CO_2 Adsorption Ability

metal−organic frameworks	CO_2 capture (mmol/g)	pressure/temperature
Cu-BTT[21,22]	0.277	low pressure
Cu-BTTri-en[21,22]	0.366	low pressure
a mixed-matrix membrane of MIL-53[23]	6	25 bar
Ln-MOF1 (Ln = Sm)[5]	1.29	1 atm/273 K
Ln-MOF2 (Ln = Gd)[5]	1.87	1 atm/273 K
1-Ln (Ln = Eu)[24]	∼1.52	1 atm/298 K
CPM-200-Fe/Mg[25]	9.27	273 K
IRH-1 (La)[26]	2.6	1 bar/298 K
IRH-2 (Ce)[26]	3.1	1 bar/298 K
IRH-3 (Pr)[26]	2.8	1 bar/298 K

Metal−organic frameworks with low-connected metallic centers, such as 3-, 4-, and 6-connected topologies, have been extensively studied; however, the number of case studies on highly connected networks are comparatively few.[5,6]

Nevertheless, lanthanide-based MOFs, because of their rich coordination geometry, ability to form highly connected lattices, high stability, and other fascinating properties, have garnered particular interest. Currently, Ln-based MOFs, with[12−29] metallic clusters and highly connected topologies such as 20-connected uninodal clusters,[5] are being studied. Ln-MOFs [Ln = Sm (MOF**1**)/Gd (MOF**2**)] of such 20-c metal−organic frameworks, with a type I isotherm and micropores, show 1.29 isotherm/g (for MOF**1** with BET surface area = 946.74 m^2/g) and 1.87 mmol/g (for MOF**2** with BET surface area = 834.26 m^2/g) CO_2 adsorption at 273 K and 1 atm.[5]

Another Ln-MOF (Ln = Eu) with ether O-decorated polycarboxylic acid linkers shows isotherm type I and 34.1 cm^3/g (∼1.52 mmol/g) CO_2 adsorption under 1 atm pressure

https://doi.org/10.1021/acsomega.3c01616
ACS Omega 2023, 8, 22742−22751

at 298 K.[30] A tricarboxylated Ln-MOF (Ln = Tb), which is thermally stable up to 440 °C with a type I isotherm and micropores, shows CO_2 capture values as high as 38.21 cm^3/g (~1.70 mmol/g) and 33.10 cm^3/g (~1.48 mmol/g) under 1 bar at 273 and 295 K, respectively. In this case, an adsorption process could be introduced as a host−guest interaction, especially in micropores. In Tb-MOF, imidazolyl open active sites and unsaturated metallic sites in the lattice could induce an electrical field to create an electric dipole in CO_2 and cause host−guest adsorption.[31−33]

La-based MOFs, which were studied by Lama et al., consist of oxygen atoms in the inner lining/walls. These oxygen atoms belong to the organic network and not the coordination group. This La-based MOF is thermally stable up to 400 °C and its desolvated form reversibly and readily adsorbs 23 cm^3/g (~1.026 mmol/g) CO_2 at 273 K. In this MOF, each metal has an LaO_9 geometry.[34]

CO_2 could be adsorbed by metal-center sites, and, depending on the structures of ligands, could be adsorbed by organic linkers, micropores, or microchannels.[26]

Recently, physisorption-based CO_2 capture with methods of (I) temperature-swing adsorption, (II) pressure-swing adsorption, and (III) vacuum-swing adsorption, because of financial advantages, have become more promising methods, which have recyclability and cost-effectiveness as their key features.[35]

To design metal−organic frameworks with increased CO_2 adsorption capability as well as improved selectivity, three guidelines should be followed during designing and production: (1) ultrahigh microporous MOFs, (2) MOFs with open metal sites, and (3) MOFs with amine functionalization.[36]

Hon et al. reported that there is strong binding between oxygen atoms of the organic linker and carbon atoms of CO_2, as well as between oxygen atoms of CO_2 and metal ions.[37] Narrow micropores in adsorbent materials (~ 0.8 nm) represent the ideal size of pores for CO_2 adsorption.[2]

Metal−organic frameworks with coordinatively unsaturated metal ions with partial positive charges on the metal sites have the advantage of Lewis acidity. Consequently, a high heat of CO_2 adsorption (Q_{st}), even at low pressure, is one of the results. High polarizability and a large quadrupole moment of CO_2 in comparison with other symmetric gas molecules, such as N_2, cause strong electrostatic interactions with such metal centers. These MOFs exhibit thermodynamically and kinetically desirable CO_2 adsorption. The binding mode and accessibility of CO_2 to metal atoms in these metal−organic frameworks are often end-on. Also, heteroatoms that are incorporated within the backbone of frameworks, in some cases, may exhibit strong interactions with CO_2.[38]

A stable CO_2-philic membrane with a high loading of poly(ethylene oxide), a desirable CO_2-philic compound, as a component polymer, through one-step synthesis, was prepared. The selectivities of this polymeric membrane for CO_2/N_2 and CO_2/H_2 at high pressure (20 bar) were about 36 and 21, respectively.[39,40]

Materials that are used in the industry should have a stable shape and be easy to handle. Shaped materials are more ready to use, and composites and multicomponent materials are considered the most prominent and well-known category of such compounds by some researchers.

A kind of diamine-functionalized MOF as a desirable CO_2 adsorbent was combined with poly(vinylidene fluoride) (PVDF) to prepare an MOF/polymer humidity-stable composite with long-term performance and structural stability by Park et al.[41] Another thermally stable, durable, and strong MOF on the mesoporous cellulose template of balsa wood was prepared by Wang and co-workers, which could adsorb 1.46 mmol/g CO_2 at atmospheric pressure and 25 °C.[42]

Composite nanofibers are from the class of shaped materials that are usually in the form of membranes. They have many advantages, including flexibility and nano-sized components, and the components could have synergistic effects. Recently, Haleem et al. reported a type of biochar-based nanofiber composed of polyvinyl alcohol (PVA), which exhibited a CO_2 adsorption ability as high as 462 mg/g.[43] Also, Othman et al. synthesized and optimized activated carbon nanofibers by incorporating magnesium oxide, which improved the amount of CO_2 uptake in comparison with other MgO/activated carbon composites at 298 K and 1 bar (from 49 to 61 cm^3/g).[44,45]

Among composite membrane materials, because of their extraordinary porous features, metal−organic frameworks have excellent properties and a wide range of functions and special position in the science. Accordingly, attention has been directed toward these materials as one of the composite components of CO_2-adsorbent membranes.

Chae et al. introduced a moisture-tolerant metal−organic framework composite membrane (epn-MOF 80@SBS) by applying a hydrophobic polymer (SBS), which could adsorb as much as 2.8 mmol/g CO_2 at 1000 ppm with considerable recyclability.[46] Also, thermal stability and water tolerance are some features of a polyacrylate (PA)−MOF composite with 1.44 mol/kg CO_2 uptake, which was synthesized by Guo et al. in the kilogram scale[47]

Likewise, He et al. tried to prepare a high-grown metal−organic framework within a mixed matrix membrane for efficient carbon capture.[48] Another mixed matrix membrane was reported by Zhu et al. They used an adhered polyphenol mediator to modify polymer chains and MOF structures, resulting in enhanced membrane carbon capture.[49]

With this background, our group tried to prepare a shaped La-TMA MOF as an electrospun composite membrane and assess its CO_2 adsorption capability.

2. MATERIALS AND METHOD

2.1. Materials and Instruments. All of the chemicals and solvents were of analytical grade and obtained from commercial sources. They were used without further purification. Benzene-1,3,5-tricarboxylic acid, $La(NO_3)_3 \cdot 6H_2O$, and Nylon 6,6 were purchased from Sigma-Aldrich company. Dimethyl formamide (DMF), formic acid, and other solvents were obtained from Merck company.

Analysis of pores in the structure, BET assessments, nitrogen adsorption/desorption graphs, and corresponding data analyses were performed using BELSORP-mini II. The morphology of the materials and their size histogram plots were analyzed by the field-emission scanning electron microscopy (FE-SEM) approach using QUANTA FEG 450 FEI as well as FE-SEM TESCAN MIRA III instruments.

X-ray diffraction patterns of the Nylon 6,6/La-TMA MOF in three different θs angles (5, 7, and 10°) were obtained using an ASENWARE, AW-XDM 300, device with step time = 1s, step size = 0.05°, 2θ = 10−80°, and θs = 5, 7, and 10°, with the grazing incidence of the thin film at 0.154184 nm wavelength, 30 mA, and 40 kV.

https://doi.org/10.1021/acsomega.3c01616
ACS Omega 2023, 8, 22742−22751

Table 3. Percentage of CO_2 Adsorption (%A) and Adsorption Capacity of Pure La-TMA MOF and the Nylon 6,6/La-TMA MOF Core/Shell Nanofiber Composite

type of materials	%A (% adsorption)	Ag (mmol CO_2/g of adsorbent)
La-TMA MOF (white powder)	43.060	0.277
Nylon 6,6/La-TMA MOF core/shell nanofiber composite	48.524	0.219

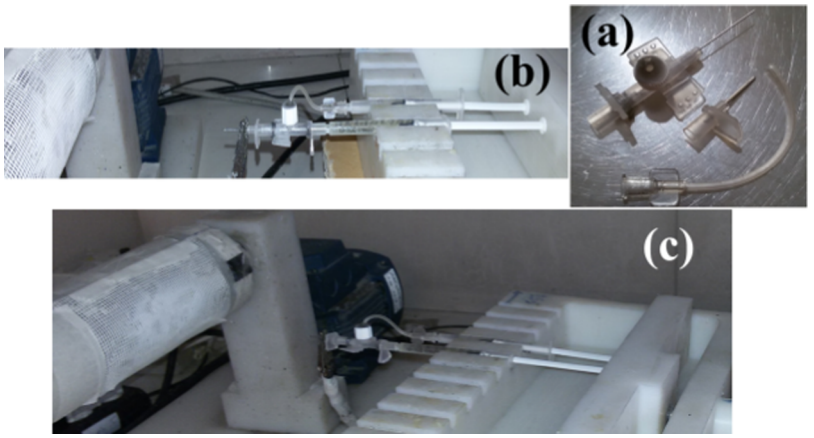

Figure 1. (a) Components of the coaxial needle with 22 and 16 G needles. (b) Coaxial electrospinning system. (c) Enlarged image of the coaxial electrospinning system.

2.2. Synthesis of La-TMA MOF. La-TMA MOF preparation was performed according to a previous study;[50] the method is described in detail here:

Trimesic acid or benzene-1,3,5-tricarboxylic acid (0.350 g, 1.67 mmol) and $La(NO_3)_3{\cdot}6H_2O$ (0.723 g, 1.67 mmol) with 1:1 molar ratio, as well as DMF (25 mL) and formic acid (25 mL), were added to an autoclavable glass flask and placed in an oven at 100 °C temperature for 12 h. After that, the flask was brought out from the oven and kept with its solvents at room temperature for 20 h. The obtained product was filtered through a filter paper and washed with 20 mL of pure DMF, 20 mL of deionized water, and 20 mL of pure acetone, respectively. Thereupon, the white precipitate was dried in an oven at 100 °C for 5 min and stored in the air under ambient conditions (of course without any additional pollution).

2.3. Preparation of Nylon 6,6 Nanofibers. In order to achieve a desirable substrate for the shaping of the metal−organic framework, Nylon 6,6 was selected, which is a heat-stable polymer (more than 400 °C).[18] To attain an optimal morphology and nano-sized diameters, a 22% (w/w) solution of Nylon 6,6 in formic acid was used. Nylon 6,6 pellets (0.22 g) were dissolved in formic acid (1 g) by vigorously stirring at room temperature for about 90 min. The distance between the needle and the collector was 10 cm. The rate of flow was 0.2 mL/h, and the voltage was 21 kV. After the beginning of electrospinning and for about 5 min, uniform nanofibers were obtained (Figure 3). Single-needle (22 G) electrospinning was applied.

2.4. Production of the Polymeric Nanofiber Composite of Nylon 6,6/La-TMA MOF Core/Shell Using Concomitant Electrospinning. In this approach, a coaxial needle (16 and 22 G) is used. The polymeric solution of Nylon 6,6 in a 1 ml syringe was directly connected to the central and minor needle (22 G); also, the suspension of La-TMA MOF in formic acid in another 1 ml syringe was connected to the major needle (16 G), which formed the shell of the polymeric fibers. Nylon 6,6 pellets (0.446 g) in formic acid (2 g) were vigorously stirred (a 22%, w/w, solution) for 75 min at room temperature. This solution was supplied by the central needle. The other solution, which was prepared from La-TMA MOF (0.02 g) and formic acid (1 mL) by simply shaking (a 2%, w/v, solution), supplied the syringe forming the shell. The distance between the coaxial needles was 10 cm, the rate of flow was 0.2 ml/h, and the voltage was 21 kV. For the easy removal of the nanofiber-produced layer from aluminum foil, a flexible lattice network was used on the surface of the Al foil. After 3 h, the product was facilely removed from the polymeric lattice network (Figure 5); immediately after electrospinning, 0.0446 g of the nanofiber composite was obtained.

2.5. Degassing Procedure of La-TMA MOF and the Nanofiber Composite. In order to desiccate and remove all of the gases from the pores of all products, all of the MOF and nanofiber materials were placed in a vacuum oven (0.1 atm) at 80 °C for 10 h in open glass flasks. Then, they were brought out from the oven and immediately covered to inhibit any gas or moisture adsorption; consequently, a slight decrease in weight is observed.

2.6. CO_2 Adsorption. To evaluate the CO_2 adsorption ability of La-TMA MOF and the core/shell mixed material membrane comprising Nylon 6,6 and La-TMA MOF nanocomposites, an encasement with a CO_2sensor was designed, fabricated, and inserted into it. A gas tube was inserted to inject CO_2(g) through it. Furthermore, MATLAB software was used to probe the CO_2 adsorption by means of a gas sensor. In order to determine the CO_2 adsorption capability of all of the materials and record the baseline, 0.6 mL of CO_2 gas was directly injected into the 80 mL encasement (which was called the "A" area). After a few seconds, when a stable condition was achieved, the maximum point of the diagram (ppm) was recorded as the concentration of CO_2(g) in area "A". Then, for every trial, to determine the CO_2 adsorption of each sample, an exact mass of that sample was placed at the end and inside of 5 mL syringe ("B" area). Then, 0.6 mL of CO_2 was injected into the "B" area to pass over the surface of materials and adsorb or

https://doi.org/10.1021/acsomega.3c01616
ACS Omega 2023, 8, 22742−22751

maybe penetrate beside/into the materials. After that, the remaining CO_2 was redirected into the "A" encasement and detected. The results of these stages are presented in Table 3.

The coaxial needle that was applied for core/shell electrospinning was easily prepared by our group. The metallic parts of two angiocaths (22 and 16 G) as well as the tube of one scalp vein were enough to prepare a cheap and simple coaxial needle (Figure 1a). Figure 1b, c, shows the system used for electrospinning in this work.

3. RESULTS AND DISCUSSION

3.1. Investigation of Carbon dioxide Adsorption. Examination of carbon dioxide adsorption of all materials was performed under usual laboratory conditions (the temperature and pressure were 27 °C and 0.815 atm, respectively). All materials were degassed in a vacuum oven at 80 °C and 0.1 atm for 10 h. If all gases are assumed as ideal gases, according to formula 1, 1 mole of CO_2(g) under our laboratory conditions is equal to 30.21976 L. In the Avogadro formula, the parameters P, V, n, and T represent pressures (atm), volume (liter), number of moles (n), and temperatures (K), respectively.[51] Under STP conditions, 1 mole of ideal gas is equal to 22.4136 L

$$P_1V_1/n_1T_1 = P_2V_2/n_2T_2 \quad (1)$$

Using the amount of remaining CO_2(g), which was entered into the "A" area after the adsorption stage (V_a), the total content of "A" encasement (V_A), and the numerical result of the gas sensor (ppm) that was probed by MATLAB software, the correlation given in formula 2 can be deduced

$$M = V_a/V_A \times 10^6 \text{ or } V_a = MV_A \times 10^6 \quad (2)$$

We can use formula 3 to calculate the percentage of CO_2 adsorption (%A) by the materials. The total starting CO_2(g) amount that was directly injected into the "A" encasement (V_{CA}) was 0.6 mL. The amount of remaining CO_2(g) that was passed over the adsorbents (V_a) was the other parameter.

$$\%A = V_{CA} - V_a/V_{CA} \times 100 \quad (3)$$

Moreover, the gas adsorption of adsorbent materials (mmol of CO_2 adsorbed under ideal conditions per gram of adsorbent material (S) under the common conditions in our laboratory (A_g)) could be calculated using formula 4

$$A_g = (V_{CA} - V_a)/(S \times 30.21976) \quad (4)$$

3.2. Nitrogen Adsorption/Desorption Isotherm and Surface Area. According to the IUPAC classification, a type IV isotherm was obtained for the Nylon 6,6/La-TMA MOF nanocomposite, and the adsorption/desorption isotherm exhibited an H3 hysteresis loop (Figure 2). Thus, mesopores exist in this nanocomposite, and thus, Nylon 6,6/La-TMA MOF is classified as a mesoporous material.[52,53] The surface area of the composite was determined through the nitrogen uptake and applying BET calculations. BET, Longmuir, BJH, t plots, and other data were computed through different approaches (Table 4). Consequently, BET and Langmuir surface areas of this nanocomposite are found to be 14.492 and 18.001 m^2/g, respectively; also, the mean pore diameter is 18.514 nm.

The nitrogen gas adsorption/desorption diagram of the nanocomposite membrane at 77 K (Figure 2) exhibits a type IV isotherm as well as H3 hysteresis. Therefore, the

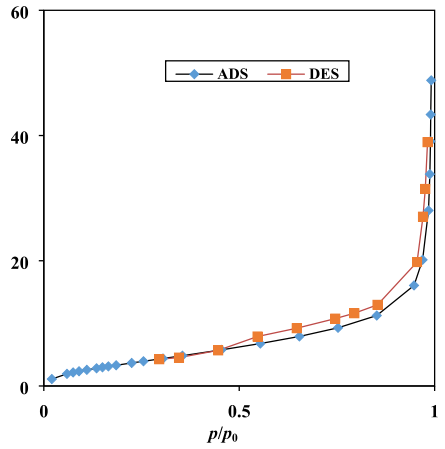

Figure 2. Nitrogen adsorption/desorption diagram of Nylon 6,6/La-TMA MOF.

Table 4. BET, Langmuir, *t*, and BJH Plots of the Nylon 6,6/La-TMA MOF Core/Shell Nanofiber Composite

BET plot		
V_m	3.3297	[cm^3(STP) g^{-1}]
$a_{s,BET}$	14.492	[m^2 g^{-1}]
mean pore diameter	18.514	[nm]
Langmuir plot		
V_m	4.1358	[cm^3(STP) g^{-1}]
$a_{s,Lang}$	18.001	[m^2 g^{-1}]
t plot adsorption branch		
a_1	6.4737	[m^2 g^{-1}]
V_1	0	[cm^3 g^{-1}]
BJH plot adsorption branch		
V_p	0.068514	[cm^3 g^{-1}]
$r_{p,peak}$(area)	1.21	[nm]
a_p	18.172	[m^2 g^{-1}]

nanocomposite membrane has mesoporous. This fact was also confirmed by BET plot calculations with a mean pore diameter of 18.514 nm (Table 4). Also, pure microtubes of La-TMA MOF show a type IV isotherm and H1 hysteresis[50] with uniform/narrow mesopores.[54] Nevertheless, a clear decrease in the mean pore diameter of the nanocomposite membrane is observed (from 41.532 to 18.514 nm).

3.3. SEM and Histogram. Field-emission scanning electron microscopy was performed to analyze in detail the surface and morphology of the Nylon 6,6 nanofibers and Nylon 6,6/La-TMA MOF nanocomposites. As exhibited in Figure 3, very uniform nanofibers, without any aggregation, were prepared using simple single-needle electrospinning. As a result of simultaneous core/sell electrospinning of Nylon 6,6 and MOF nanoparticles, nanodimensional La-TMA MOF particles on the nanofibers of Nylon 6,6 were fabricated and can be clearly seen in Figure 4 Figure 5 displays an image of Nylon 6,6/La-TMA MOF on the polymeric lattice network.

The most probable size distribution of MOF nanoparticles that were deposited on nanofibers was between 40 and 175 nm, and the peak was at 70 nm (Figure 6). Moreover, the histogram of nanofibers in this composite (Figure 7) shows the most average domain size between 50 and 200 nm (the peak at 125 nm).

3.4. Interpretation of the XRD Patterns of the Nylon 6,6/La-TMA MOF Nanocomposite. XRD grazing incidence

https://doi.org/10.1021/acsomega.3c01616
ACS Omega 2023, 8, 22742−22751

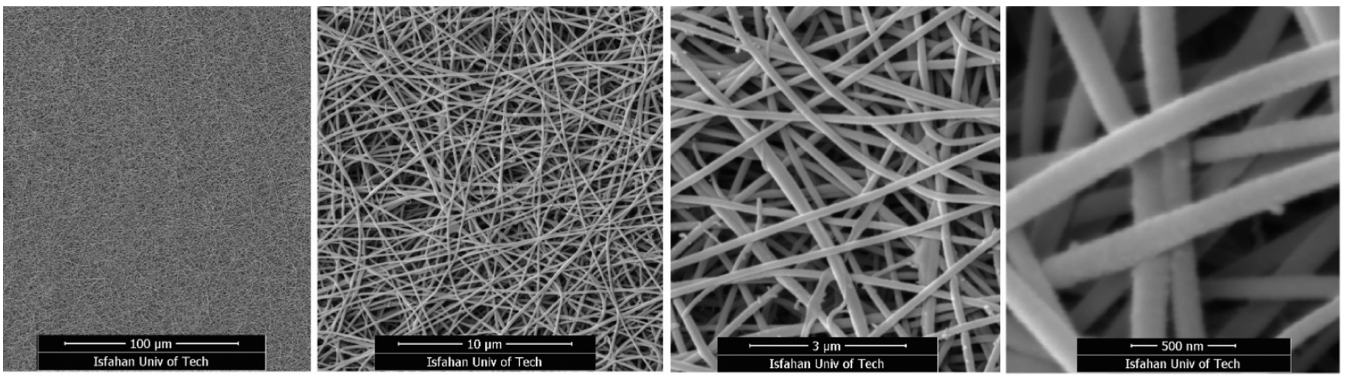

Figure 3. Morphology of uniform fibers of Nylon 6,6.

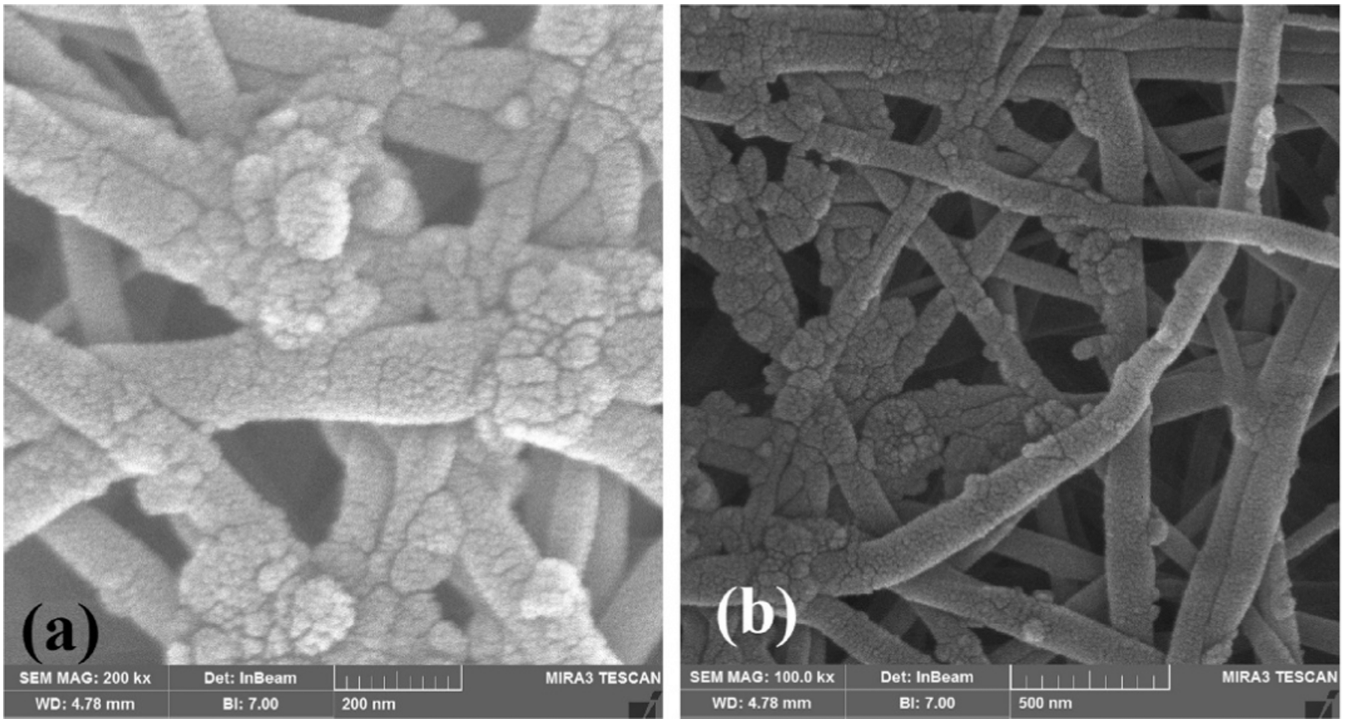

Figure 4. (a and b) Morphology of Nylon 6,6/La-TMA MOF composite nanofibers.

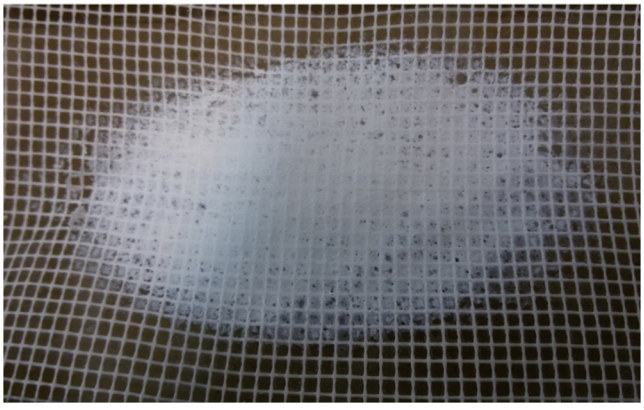

Figure 5. Image of Nylon 6,6/La-TMA MOF on the polymeric lattice network.

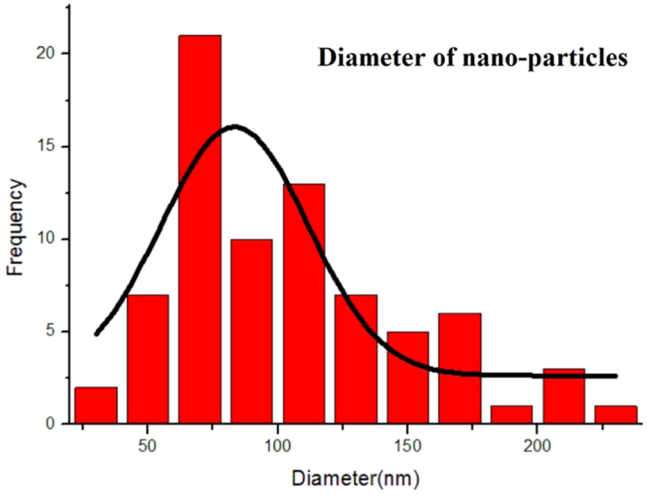

Figure 6. Histogram or size distribution of MOF nanoparticles in Nylon 6,6/La-TMA MOF.

patterns of the Nylon 6,6/La-TMA MOF reveal the presence of amorphous and crystalline phases together in the nanocomposite. The hilly broad peak in the background and several

https://doi.org/10.1021/acsomega.3c01616
ACS Omega 2023, 8, 22742−22751

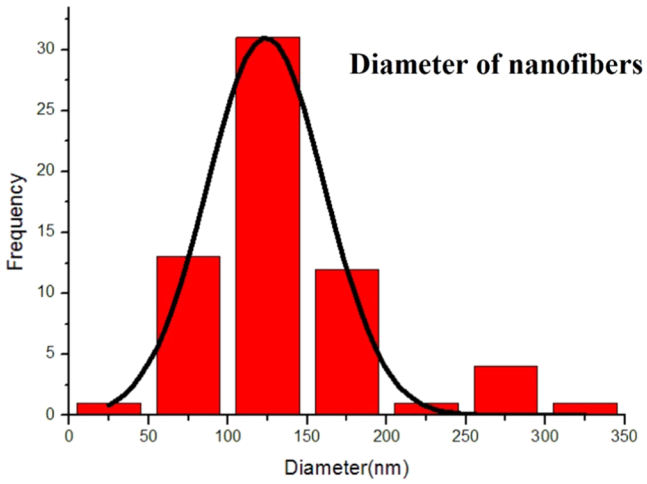

Figure 7. Histogram or size distribution of nanofibers in Nylon 6,6/La-TMA MOF.

small peaks or microstrains are attributed to polymeric Nylon 6,6 and nanoparticles of MOF, respectively (Figure 8). This hilly broad peak of amorphous polymer overlaps with some peaks of La-TMA MOF in this area. The normal XRD pattern of microhexagonal hollow tubes of La-TMA MOF has been reported in the literature. The XRD pattern of La-TMA micro-MOF, according to the micro-sized and desirable crystallinity, was optimized.[50] Furthermore, the Nylon 6,6/La-TMA MOF nanocomposite in the form of a thin film was studied throughout grazing incidence at θs = 5, 7, and 10°. It is noticeable that due to a decrease in the size of MOF particles (the micro-size changed into nano-size), microstrains instead of sharp peaks appear.[55,56]

4. CONCLUSIONS

In summary, in this work, uniform and bead-free nanofibers of a Nylon 6,6 electrospun membrane were prepared. Then, La-TMA MOF was used in the nanoparticle form as a particle shell of Nylon 6,6. By using the electrospinning approach, the flexible core/shell Nylon 6,6/La-TMA MOF membrane was prepared. The morphology, nano-size, and composite structure of Nylon 6,6 nanofibers were confirmed by FE-SEM images and XRD grazing incidence patterns. FE-SEM, surface area calculations, nitrogen adsorption/desorption diagrams, XRD grazing incidence patterns of the nanocomposite thin-film membrane, and histogram plots of the Nylon 6,6/La-TMA MOF were applied to confirm the MOF nanoparticles on the nanofiber structure and the size distribution of the components.

Regarding the gas adsorption of metal−organic frameworks or any other catalyst, "how to shape the catalyst to be used as a gas adsorbent?" is a vital question. Consequently, a major part of our project was directed toward finding an answer to this question.

As it was clearly clarified, "shaping" of the lanthanum-TMA MOF was considered by our group. In this project, by a facile approach, nano La-TMA MOF particles were deposited on the surface of Nylon 6,6 spun nanofibers to produce a core/shell nanocomposite product. Besides using pure La-TMA MOF, for the first time, the carbon dioxide adsorption by this mixed membrane texture was examined, and the performances are reported (0.277 and 0.219 mmol/g, respectively); the synthesis of the nanocomposite membrane from microtubes of La-TMA MOF increased the %A of the micro La-TMA MOF (% 43.060) to %48.524 for the Nylon 6,6/La-TMA MOF.

As shown in Table 3, the CO_2 adsorption abilities of La-TMA MOF and a novel electrospinning mixed membrane core/shell Nylon 6,6/La-TMA MOF nanocomposite were assessed. Although the removal of phosphate and fluoride from water[57,58] had been examined by using lanthanum metal−organic frameworks with a trimesic acid linker, carbon dioxide adsorption had not been taken into account by applying La-TMA MOFs in previous studies. The linkage between "Nylon 6,6" and "La-TMA MOF" is a type of strong physical binding. Therefore, changes in its chemical properties are not expected. The thermal stabilities of "Nylon 6,6" and "La-TMA MOF" are 424 °C[18] and about 400 °C,[50] respectively. Consequently, the thermal stability of the composite membrane is about 400 °C.

The adsorption performances of some classes of metal−organic frameworks are inherently limited by their size, functionality, pore structures, and so on, which would be correlated with the amount of gas uptake. The functionalities of organic linkers and features of pores are the main parameters that should be considered to manage and improve the gas adsorption of adsorbents.

A single type of organic linker and organic node leads to the simplicity of the framework and pore architecture of La-TMA MOF.

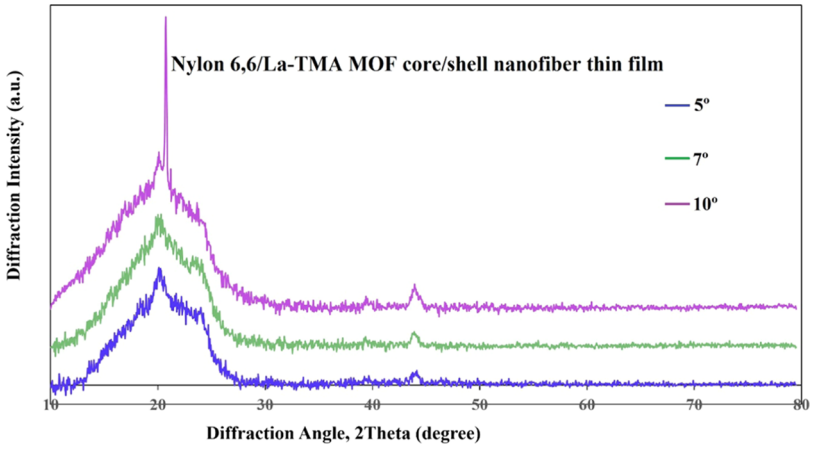

Figure 8. XRD grazing incidence thin-film patterns of Nylon 6,6/La-TMA MOF at θs = 5, 7, and 10°.

https://doi.org/10.1021/acsomega.3c01616
ACS Omega 2023, 8, 22742−22751

The nitrogen gas adsorption/desorption diagram of the nanocomposite membrane at 77 K (Figure 2) exhibits a type IV isotherm as well as H3 hysteresis. Therefore, the nanocomposite membrane has mesopores. This fact was also confirmed by BET plot calculations, with a mean pore diameter of 18.514 nm. Also, pure microtubes of La-TMA MOF exhibit a type IV isotherm and H1 hysteresis[50] with uniform/narrow mesopores.[54]

In spite of the mesoporous nature of La-TMA MOF (mean pore diameter 41.532 nm in the BET plot) and Nylon 6,6/La-TMA MOF (mean pore diameter 18.514 nm in the BET plot), the size of mesopores considerably decreased as a result of core/shell electrospinning of the composite membrane and incorporation of Nylon6,6 nanofibers. However, the presence of micropores of the desired size for CO_2 capture, below 2 nm,[13] and in the ideal state, 0.8 nm,[2] would increase the amount of CO_2 capture.

Furthermore, the flexibility and thermal stability of the membrane (more than 400 °C) are other advantages of the composite membrane.

High-coordinated metal sites of La-TMA MOF, because of the presence of the lanthanide element, as well as the oxygen heteroatom, could improve the CO_2 uptake. Incorporation of the MOF into a polymeric electrospun membrane could have synergistic effects on the shaped product.

As a result of the preparation of the nanocomposite membrane from microtubes of La-TMA MOF, the %A of the micro La-TMA MOF (% 43.060) increased to %48.524 for Nylon 6,6/La-TMA MOF.

These results show that the CO_2 capture by this method could be extended to other adsorbent materials and polymeric fibers of this group to improve the ability of CO_2 adsorption by using the electrospun fiber technology and composite membranes.

■ ASSOCIATED CONTENT

Supporting Information

The Supporting Information is available free of charge at https://pubs.acs.org/doi/10.1021/acsomega.3c01616.

XRD peak data of the Nylon 6,6/La-TMA MOF core/shell composite are given in detail in the Supporting Information file (PDF)

■ AUTHOR INFORMATION

Corresponding Author

Zohreh Fateminia − *Department of Chemistry, Isfahan University of Technology, Isfahan 84156-83111, Iran;* orcid.org/0000-0002-7952-6245; Email: z.fateminia@ch.iut.ac.ir

Authors

Hossein Chiniforoshan − *Department of Chemistry, Isfahan University of Technology, Isfahan 84156-83111, Iran*

Vahid Ghafarinia − *Department of Electrical and Computer Engineering, Isfahan University of Technology, Isfahan 84156-83111, Iran*

Complete contact information is available at: https://pubs.acs.org/10.1021/acsomega.3c01616

Funding

Hossein Chiniforoshan: funding acquisition, project administration, resources, and visualization. **Vahid Ghafarinia**: funding acquisition, project administration, resources, and methodology. **Zohreh Fateminia**: data curation, formal analysis, investigation, methodology, and writing.

Notes

The authors declare no competing financial interest.

■ ACKNOWLEDGMENTS

The authors acknowledge financial support from Isfahan University of Technology (IUT).

■ ABBREVIATIONS

STPstandard temperature and pressures; PMMApoly(methyl methacrylate); PVCpoly(vinyl chloride)

■ REFERENCES

(1) Naseer, M. N.; Zaidi, A. A.; Dutta, K.; Wahab, Y. A.; Jaafar, J.; Nusrat, R.; Ullah, I.; Kim, B. Past, present and future of materials' applications for CO_2 capture: A bibliometric analysis. *Energy Rep.* **2022**, *8*, 4252−4264.

(2) Shaki, H. The use of electrospun nanofibers for absorption and separation of carbon dioxide: A review. *J. Ind. Text.* **2023**, *53*, No. 152808372311602.

(3) Nagra, S. S.; Armstrong, D. A. Mechanism of Electron Capture and Hydrogen Formation by HBr Irradiated in Mixtures with C_2F_6, CO_2, and Xe. *Can. J. Chem.* **1975**, *53*, 3305−3312.

(4) Li, H.; Eddaoudi, M.; Groy, T. L.; Yaghi, O. M. Establishing microporosity in open metal− organic frameworks: gas sorption isotherms for Zn (BDC)(BDC = 1, 4-benzenedicarboxylate). *J. Am. Chem. Soc.* **1998**, *120*, 8571−8572.

(5) Ugale, B.; Dhankhar, S. S.; Nagaraja, C. M. Exceptionally stable and 20-connected lanthanide metal−organic frameworks for selective CO_2 capture and conversion at atmospheric pressure. *Cryst. Growth Des.* **2018**, *18*, 2432−2440.

(6) Trickett, C. A.; Helal, A.; Al-Maythalony, B. A.; Yamani, Z. H.; Cordova, K. E.; Yaghi, O. M. The chemistry of metal−organic frameworks for CO_2 capture, regeneration and conversion. *Nat. Rev. Mater.* **2017**, *2*, 17045.

(7) Seoane, B.; Coronas, J.; Gascon, I.; Benavides, M. E.; Karvan, O.; Caro, J.; Kapteijn, F.; Gascon, J. Metal−organic framework based mixed matrix membranes: a solution for highly efficient CO_2 capture? *Chem. Soc. Rev.* **2015**, *44*, 2421−2454.

(8) Liu, S.; Liu, J.; Hou, X.; Xu, T.; Tong, J.; Zhang, J.; Ye, B.; Liu, B. Porous liquid: a stable ZIF-8 colloid in ionic liquid with permanent porosity. *Langmuir* **2018**, *34*, 3654−3660.

(9) Cong, H.; Radosz, M.; Towler, B. F.; Shen, Y. Polymer−inorganic nanocomposite membranes for gas separation. *Sep. Purif. Technol.* **2007**, *55*, 281−291.

(10) Baker, R. W.; Lokhandwala, K. Natural gas processing with membranes: an overview. *Ind. Eng. Chem. Res.* **2008**, *47*, 2109−2121.

(11) Chung, T. S.; Jiang, L. Y.; Li, Y.; Kulprathipanja, S. Mixed matrix membranes (MMMs) comprising organic polymers with dispersed inorganic fillers for gas separation. *Prog. Polym. Sci.* **2007**, *32*, 483−507.

(12) Li, J. R.; Kuppler, R. J.; Zhou, H. C. Selective gas adsorption and separation in metal−organic frameworks. *Chem. Soc. Rev.* **2009**, *38*, 1477−1504.

(13) Cheng, Y.; Ying, Y.; Japip, S.; Jiang, S. D.; Chung, T. S.; Zhang, S.; Zhao, D. Advanced porous materials in mixed matrix membranes. *Adv. Mater.* **2018**, *30*, No. 1802401.

(14) Ryan, J. J.; Casalini, R.; Orlicki, J. A.; Lundin, J. G. Controlled release of the insect repellent picaridin from electrospun nylon-6, 6 nanofibers. *Polym. Adv. Technol.* **2020**, *31*, 3039−3047.

(15) Parlayıcı, Ş.; Avcı, A.; Pehlivan, E. Electrospinning of polymeric nanofiber (nylon 6, 6/graphene oxide) for removal of Cr (VI): synthesis and adsorption studies. *J. Anal. Sci. Technol.* **2019**, *10*, 13.

(16) Ji, W.; Wang, X.; Ding, T.; Chakir, S.; Xu, Y.; Huang, X.; Wang, H. Electrospinning preparation of nylon-6@ UiO-66-NH_2 fiber

membrane for selective adsorption enhanced photocatalysis reduction of Cr (VI) in water. *J. Chem. Eng.* **2023**, *451*, No. 138973.
(17) Keirouz, A.; Radacsi, N.; Ren, Q.; Dommann, A.; Beldi, G.; Maniura-Weber, K.; Rossi, R. M.; Fortunato, G. Nylon-6/chitosan core/shell antimicrobial nanofibers for the prevention of mesh-associated surgical site infection. *J. Nanobiotechnol.* **2020**, *18*, 1−17.
(18) Carrizales, C.; Pelfrey, S.; Rincon, R.; Eubanks, T. M.; Kuang, A.; McClure, M. J.; Bowlin, G. L.; Macossay, J. Thermal and mechanical properties of electrospun PMMA, PVC, Nylon 6, and Nylon 6, 6. *Polym. Adv. Technol.* **2008**, *19*, 124−130.
(19) Liu, Y.; Wang, Z. U.; Zhou, H. C. Recent advances in carbon dioxide capture with metal-organic frameworks. *Greenhouse Gases: Sci. Technol.* **2012**, *2*, 239−259.
(20) Sumida, K.; Rogow, D. L.; Mason, J. A.; McDonald, T. M.; Bloch, E. D.; Herm, Z. R.; Bae, T. H.; Long, J. R. Carbon dioxide capture in metal−organic frameworks. *Chem. Rev.* **2012**, *112*, 724−781.
(21) Demessence, A.; D'Alessandro, D. M.; Foo, M. L.; Long, J. R. Strong CO_2 Binding in a Water-Stable, Triazolate-Bridged Metal−Organic Framework Functionalized with Ethylenediamine. *J. Am. Chem. Soc.* **2009**, *131*, 8784−8786.
(22) McDonald, T. M.; D'Alessandro, D. M.; Krishna, R.; Long, J. R. Enhanced Carbon Dioxide Capture upon Incorporation of N,N-[Prime or Minute]-Dimethylethylenediamine in the Metal-Organic Framework CuBTTri. *Chem. Sci.* **2011**, *2*, 2022.
(23) Zornoza, B.; Martinez-Joaristi, A.; Serra-Crespo, P.; Tellez, C.; Coronas, J.; Gascon, J.; Kapteijn, F. Functionalized flexible MOFs as fillers in mixed matrix membranes for highly selective separation of CO_2 from CH_4 at elevated pressures. *Chem. Commun.* **2011**, *47*, 9522−9524.
(24) Ma, L. N.; Liu, Y.; Li, Y. Z.; Hu, Q. X.; Hou, L.; Wang, Y. Y. Three Lanthanide Metal-Organic Frameworks Based on an Ether-Decorated Polycarboxylic Acid Linker: Luminescence Modulation, CO_2 Capture and Conversion Properties. *Chem. Asian J.* **2020**, *15*, 191−197.
(25) Zhai, Q. G.; Bu, X.; Mao, C.; Zhao, X.; Feng, P. Systematic and dramatic tuning on gas sorption performance in heterometallic metal−organic frameworks. *J. Am. Chem. Soc.* **2016**, *138*, 2524−2527.
(26) Mohan, M.; Essalhi, M.; Durette, D.; Rana, L. K.; Ayevide, F. K.; Maris, T.; Duong, A. A rational design of microporous nitrogen-rich lanthanide metal−organic frameworks for CO_2/CH_4 separation. *ACS Appl. Mater. Interfaces* **2020**, *12*, 50619−50627.
(27) Xue, D. X.; Belmabkhout, Y.; Shekhah, O.; Jiang, H.; Adil, K.; Cairns, A. J.; Eddaoudi, M. Tunable rare earth fcu-MOF platform: access to adsorption kinetics driven gas/vapor separations via pore size contraction. *J. Am. Chem. Soc.* **2015**, *137*, 5034−5040.
(28) Li, Y. J.; Wang, Y. L.; Liu, Q. Y. The highly connected MOFs constructed from nonanuclear and trinuclear lanthanide-carboxylate clusters: selective gas adsorption and luminescent pH sensing. *Inorg. Chem.* **2017**, *56*, 2159−2164.
(29) Guillerm, V.; Weseliński, ŁJ.; Belmabkhout, Y.; Cairns, A. J.; D'elia, V.; Wojtas, Ł.; Adil, K.; Eddaoudi, M. Discovery and introduction of a (3, 18)-connected net as an ideal blueprint for the design of metal−organic frameworks. *Nat. Chem.* **2014**, *6*, 673−680.
(30) Ma, L. N.; Liu, Y.; Li, Y. Z.; Hu, Q. X.; Hou, L.; Wang, Y. Y. Three Lanthanide Metal-Organic Frameworks Based on an Ether-Decorated Polycarboxylic Acid Linker: Luminescence Modulation, CO_2 Capture and Conversion Properties. *Chem. Asian J.* **2020**, *15*, 191−197.
(31) Wang, X.; Zhang, L.; Yang, J.; Liu, F.; Dai, F.; Wang, R.; Sun, D. Lanthanide metal−organic frameworks containing a novel flexible ligand for luminescence sensing of small organic molecules and selective adsorption. *J. Mater. Chem. A* **2015**, *3*, 12777−12785.
(32) Li, J. R.; Kuppler, R. J.; Zhou, H. C. Selective gas adsorption and separation in metal−organic frameworks. *Chem. Soc. Rev.* **2009**, *38*, 1477−1504.
(33) Jing, T.; Chen, L.; Jiang, F.; Yang, Y.; Zhou, K.; Yu, M.; Cao, Z.; Li, S.; Hong, M. Fabrication of a robust lanthanide metal−organic framework as a multifunctional material for Fe (III) detection, CO_2 capture, and utilization. *Cryst. Growth Des.* **2018**, *18*, 2956−2963.
(34) Lama, P.; Aijaz, A.; Neogi, S.; Barbour, L. J.; Bharadwaj, P. K. Microporous La (III) metal− organic framework using a semirigid tricarboxylic ligand: synthesis, single-crystal to single-crystal sorption properties, and gas adsorption studies. *Cryst. Growth Des.* **2010**, *10*, 3410−3417.
(35) Hu, Z.; Wang, Y.; Shah, B. B.; Zhao, D. CO_2 capture in metal−organic framework adsorbents: an engineering perspective. *Adv. Sustainable Syst.* **2019**, *3*, No. 1800080.
(36) Liu, J.; Wei, Y.; Zhao, Y. Trace carbon dioxide capture by metal−organic frameworks. *ACS Sustainable Chem. Eng.* **2019**, *7*, 82−93.
(37) Hou, X. J.; He, P.; Li, H.; Wang, X. Understanding the adsorption mechanism of C_2H_2, CO_2, and CH_4 in isostructural metal−organic frameworks with coordinatively unsaturated metal sites. *J. Phys. Chem. C.* **2013**, *117*, 2824−2834.
(38) Trickett, C. A.; Helal, A.; Al-Maythalony, B. A.; Yamani, Z. H.; Cordova, K. E.; Yaghi, O. M. The chemistry of metal−organic frameworks for CO_2 capture, regeneration and conversion. *Nat. Rev. Mater.* **2017**, *2*, 17045.
(39) Zhu, B.; He, S.; Wu, Y.; Li, S.; Shao, L. One-step synthesis of structurally stable CO_2-philic membranes with ultra-high PEO loading for enhanced carbon capture *Engineering* 2022, DOI: 10.1016/j.eng.2022.03.016.
(40) Hu, Z.; Wang, Y.; Shah, B. B.; Zhao, D. CO_2 capture in metal−organic framework adsorbents: an engineering perspective. *Adv. Sustainable Syst.* **2019**, *3*, No. 1800080.
(41) Park, J.; Chae, Y. S.; Kang, D. W.; Kang, M.; Choe, J. H.; Kim, S.; Kim, J. Y.; Jeong, Y. W.; Hong, C. S. Shaping of a Metal−Organic Framework−Polymer Composite and Its CO_2 Adsorption Performances from Humid Indoor Air. *ACS Appl. Mater. Interfaces* **2021**, *13*, 25421−25427.
(42) Wang, S.; Wang, C.; Zhou, Q. Strong foam-like composites from highly mesoporous wood and metal-organic frameworks for efficient CO_2 capture. *ACS Appl. Mater. Interfaces* **2021**, *13*, 29949−29959.
(43) Haleem, N.; Khattak, A.; Jamal, Y.; Sajid, M.; Shahzad, Z.; Raza, H. Development of poly vinyl alcohol (PVA) based biochar nanofibers for carbon dioxide (CO_2) adsorption. *Renewable Sustainable Energy Rev.* **2022**, *157*, No. 112019.
(44) Othman, F. E. C.; Yusof, N.; Samitsu, S.; Abdullah, N.; Hamid, M. F.; Nagai, K.; Abidin, M. N. Z.; Azali, M. A.; Ismail, A. F.; Jaafar, J.; Aziz, F.; Salleh, W. N. W. Activated carbon nanofibers incorporated metal oxides for CO_2 adsorption: Effects of different type of metal oxides. *J. CO_2 Util.* **2021**, *45*, No. 101434.
(45) Shahkarami, S.; Dalai, A. K.; Soltan, J. Enhanced CO_2 adsorption using MgO-impregnated activated carbon: impact of preparation techniques. *Ind. Eng. Chem. Res.* **2016**, *55*, 5955−5964.
(46) Chae, Y. S.; Park, S.; Kang, D. W.; Kim, D. W.; Kang, M.; San Choi, D.; Choe, J. H.; Hong, C. S. Moisture-tolerant diamine-appended metal−organic framework composites for effective indoor CO_2 capture through facile spray coating. *J. Chem. Eng.* **2022**, *433*, No. 133856.
(47) Guo, M.; Wu, H.; Lv, L.; Meng, H.; Yun, J.; Jin, J.; Mi, J. A highly efficient and stable composite of polyacrylate and metal−organic framework prepared by interface engineering for direct air capture. *ACS Appl. Mater. Interfaces* **2021**, *13*, 21775−21785.
(48) He, S.; Zhu, B.; Jiang, X.; Han, G.; Li, S.; Lau, C. H.; Wu, Y.; Zhang, Y.; Shao, L. Symbiosis-inspired de novo synthesis of ultrahigh MOF growth mixed matrix membranes for sustainable carbon capture. *Proc. Natl. Acad. Sci. U.S.A.* **2022**, *119*, No. e2114964119.
(49) Zhu, B.; He, S.; Yang, Y.; Li, S.; Lau, C. H.; Liu, S.; Shao, L. Boosting membrane carbon capture via multifaceted polyphenol-mediated soldering. *Nat. Commun.* **2023**, *14*, No. 1697.
(50) Fateminia, Z.; Chiniforoshan, H. Optimization and Synthesis of a La-TMA MOF with Some Improvements in Its Properties. *ACS Omega* **2023**, *8*, 262−270.

https://doi.org/10.1021/acsomega.3c01616
ACS Omega 2023, 8, 22742−22751

(51) Schmiermund, T. *The Avogadro Constant*; Springer Fachmedien Wiesbaden, 2020.
(52) Al-Ghouti, M. A.; Da'ana, D. A. Guidelines for the use and interpretation of adsorption isotherm models: A review. *J. Hazard. Mater.* **2020**, *393*, No. 122383.
(53) Horvat, G.; Pantić, M.; Knez, Ž.; Novak, Z. A Brief Evaluation of Pore Structure Determination for Bioaerogels. *Gels.* **2022**, *8*, 438.
(54) Sotomayor, F. J.; Cychosz, K. A.; Thommes, M. Characterization of micro/mesoporous materials by physisorption: concepts and case studies. *Acc. Mater. Surf. Res.* **2018**, *3*, 34−50.
(55) Widjonarko, N. E. Introduction to advanced X-ray diffraction techniques for polymeric thin films. *Coatings.* **2016**, *6*, 54.
(56) Nabok, D.; Puschnig, P.; Ambrosch-Draxl, C.; Werzer, O.; Resel, R.; Smilgies, D. M. Crystal and electronic structures of pentacene thin films from grazing-incidence X-ray diffraction and first-principles calculations. *Phys. Rev. B* **2007**, *76*, No. 235322.
(57) Zhang, X.; Sun, F.; He, J.; Xu, H.; Cui, F.; Wang, W. Robust phosphate capture over inorganic adsorbents derived from lanthanum metal organic frameworks. *Chem. Eng. J.* **2017**, *326*, 1086−1094.
(58) Jeyaseelan, A.; Kumar, I. A.; Viswanathan, N.; Naushad, M. Development and characterization of hydroxyapatite layered lanthanum organic frameworks by template method for defluoridation of water. *J. Colloid Interface Sci.* **2022**, *622*, 228.

https://doi.org/10.1021/acsomega.3c01616
ACS Omega 2023, 8, 22742−22751